

# Fluid Mechanics at the Interface between a Variable Viscosity Fluid Layer and a Variable Permeability Porous Medium

M.S. ABU ZAYTOON

Department of Mathematics University of Petra,  
Amman, JORDAN

M.H. HAMDAN\*

Department of Mathematics and Statistics,  
University of New Brunswick Saint John,  
CANADA

**Abstract:** Coupled parallel flow of fluid with pressure-dependent viscosity through an inclined channel underlain by a porous layer of variable permeability and variable thickness is initiated in this work. Conditions at the interface between the channel and the porous layer reflect continuity assumptions of velocity, shear stress, pressure and viscosity. Viscosity is assumed to vary in terms of a continuous pressure function that is valid throughout the channel and the porous layer. Model equations are cast in a form where the pressure as an independent variable and solutions are obtained to illustrate the effects of flow and media parameters on the dynamics behaviour of pressure-dependent viscosity fluid. A permeability and a viscosity adjustable control parameters are introduced to avoid unrealistic values of permeability and viscosity. This work could serve as a model for flow over a mushy zone.

**Keywords:** Coupled Parallel Flow, Pressure-Dependent Viscosity, Variable Permeability

Received: May 16, 2021. Revised: August 8, 2021. Accepted: September 5, 2021. Published: September 27, 2021.

## 1. Introduction

Recent advances in the modelling and simulation of flow through porous media include a focus on fluids with variable or stratified viscosities, and fluids with pressure-dependent viscosities, [1,2,3]. In particular, interest in fluids with pressure-dependent viscosities in porous media stems from their industrial applications in the oil industry (enhanced oil recovery and geological carbon sequestration), food and polymer processing, in the pharmaceutical industry, in fluidics and in thin film lubrication, [2, 4, 5, 6].

It is generally accepted that for some fluids, such as water, viscous stresses arising from fluid flow are proportional to the local strain at every point, and the viscous stress and the strain rate are related by a constant viscosity tensor that does not depend on the stress state and velocity of the flow. However, many fluids, such as paint and polymers exhibit behaviours in which a fluid becomes either thicker, or thinner when sheared. Fluid viscosity variations and viscosity dependence on pressure have been discussed by various authors, including Stokes [7], Barus, [8,9], Bridgman [10], Vergne [11], and Subramanian & Rajagopal [12].

Nakshatrala and Rajagopal [2] provided an account of viscosity variations which includes viscosity changes due to temperature, pressure and shear-thinning. A model describing the dependence of viscosity on pressure,

temperature and density has also been reported in Szeri [4]. Relationships describing dependence of viscosity on pressure have been suggested and tested. These relationships shed some light on the most appropriate pressure-viscosity relationships, and they compare the behaviour of the flow under different relationships, [13]. They include the exponential relationship proposed by Barus [9], as well as linear and polynomial relationships, [13-15].

Models describing the flow of fluids with pressure-dependent viscosity through porous media have been derived, discussed or analyzed by various authors, including Nakshatrala and Rajagopal, [2], Kannan and Rajagopal [13], Srinivasan and Rajagopal, [16], Chang et.al. [17], and Abu Zaytoon et.al. [18]. A number of elegant investigations and solutions to flow problems in free-space and in porous media have also been provided by various authors. Notable among these is the study of compressible flow where Housiadas and Georgiou, [19], provided new solutions for weakly compressible Newtonian Poiseuille flows with pressure-dependent viscosity. Creeping flow past a sphere for fluids with pressure-dependent viscosity was also studied by Housiadas et.al. [20]. Danish et. al. [21] provided first exact solutions for mixed boundary value problems concerning the motions of fluids with exponential dependence of viscosity on pressure. Fusi et.al. [15] provided thorough analysis of three important filtration

problems in their analysis of mathematical models for fluids with pressure-dependent viscosity flowing in porous media.

Other available solutions have been discussed in the works of Hron et.al. [22], Málek and Rajagopal [23, 24], Savatorova and Rajagopal [25] and Srinivasan et.al. [26].

Of interest to the current work is the generalized Brinkman model, [12, 13, 16], in which the flow through a rigid porous structure is described by the following equations of continuity and momentum, respectively, written here for steady flow:

$$\nabla \cdot \vec{u} = 0 \quad (1)$$

$$\rho \vec{u} \cdot \nabla \vec{u} = -\nabla p + \nabla \cdot \vec{T} - \lambda(p) \vec{u} \quad (2a)$$

where

$$\vec{T} = -p\vec{I} + 2\mu(p)\vec{A} \quad (2b)$$

is the Cauchy stress tensor in which

$$\vec{A} = \frac{1}{2} (\nabla \vec{u} + (\nabla \vec{u})^T) \quad (2c)$$

where  $\vec{u}$  is the velocity vector field,  $p$  is the pressure,  $\rho$  is the fluid density,  $\rho \vec{G} = (\rho G_1, \rho G_2, \rho G_3)$  is the body force,

$\mu = \mu(p)$  is the variable viscosity, and  $\lambda(p)$  is a drag function

that has been given various forms as discussed by Subramanian and Rajagopal, [12], and include exponential and polynomial forms in terms of pressure. In order to account for the effects of medium permeability, the drag function will be scaled, and expressed in this work as the ratio between viscosity of the fluid and permeability of the porous medium, namely,  $\lambda(p) = \mu(p)/k$ .

The above choice offers the advantage of modifying momentum equations (2a) to explicitly contain the permeability of the porous medium which, in turn, facilitates studies of flow through constant and variable permeability porous media, in a manner that was carried out by Alzahrani et.al. [27, 28] in their study of flow through an inclined porous layer. Kanaan and Rajagopal [13] provided analysis, and obtained the solution to model equations (1) and (2) in their study of flow through a porous channel inclined to the horizontal, for various forms of viscosity as a function of pressure, and for different forms of  $\lambda(p)$ .

The flow domain of a porous channel inclined to the horizontal has been a model configuration for many problems, including thin film lubrication and wave, [29], and, we believe, it facilitates the introduction of a continuous pressure function on which viscosity depends. This configuration has been used in the detailed work of Kanaan and Rajagopal [13] to provide complete and accurate results of the flow characteristics of pressure-dependent viscosity fluid flow in a porous layer. We will utilize this configuration in this work in which we

consider the coupled parallel flow of a fluid with pressure-dependent viscosity through a free-space channel underlain by a Brinkman-type porous layer. The porous layer is assumed to be of variable permeability.

While flow through channels over porous layers has received considerable attention in the porous media literature, the current work initiates its consideration when the fluid involved is a pressure-dependent viscosity fluid. To this end, we use conditions at the interface between the channel and the porous layer of variable permeability and variable thickness that emphasize continuity of pressure, viscosity, shear stress and velocity. This approach represents an extension of the continuity assumptions recommended by Rudraiah [30] when Brinkman's equation is used in a finite domain.

Little work has been carried out in the literature on flow through variable permeability porous layers [31]. This provides more motivations for this study. Hamdan and Kamel [31] introduced a variable permeability quadratic model suitable for Brinkman's equation, based on a special non-dimensionalization procedure. In the current work, we implement a variable permeability model that is also quadratic but with a form derived from the linear pressure function across the flow configuration. Model equations are expressed with the pressure as an independent variable and solved. Results are analyzed to illustrate the effects of flow and medium parameters on the flow quantities of viscosity, vorticity and shear stress. Two important parameters are introduced in this work so that one can avoid unrealistic values of permeability and viscosity, namely a permeability and a viscosity adjustable control parameters.

This manuscript is organized as follows. In Section II, we provide problem formulation and solution. In Section III, we provide detailed analysis of our computational and simulation results, and document the effects of the flow and media parameters on the flow characteristic. We close with a Conclusion that summarizes the main findings.

We reiterate here the following highlights of this work:

- It initiates the study of coupled parallel flow of fluids with pressure-dependent viscosities.
- It considers flow over variable permeability and variable thickness porous layers.
- It provides a formulation of the problem with pressure as an independent variable.
- It introduces a permeability and a viscosity adjustable control parameters to avoid unrealistic values.
- It obtains an accurate and exact solution to the flow problem in the given configuration, with detailed computations and simulations using *Maple Software Package 2020*.

## 2. Problem Formulation and Solution

The flow of an incompressible fluid with variable viscosity through a free-space channel (where we take  $\lambda(p) = 0$ ) or through a porous medium is governed by the following

continuity and momentum equations (1) and (2), above. These equations represent a system of four scalar equations in the five unknowns  $\vec{u}, p$  and  $\mu$ . It is therefore assumed that the viscosity  $\mu$  is a known function of pressure  $p$  so that the governing equations represent a determinate system of four equations in the four unknowns  $\vec{u}$  and  $p$ .

Considering that the flow domain is the configuration shown in Fig. 1, the coupled fluid is through a channel and porous layer, with the channel occupying  $h_1 \leq y \leq h$  and the porous layer occupying  $0 \leq y \leq h_1$ . The channel and porous layer are parallel and meet at a sharp interface  $y = h_1$  with angle of inclination  $\vartheta$ , and are bounded by solids walls at  $y = 0$  and  $y = h$ .

The assumption of a sharp interface in addition to the assumption of a fluid with the same density and viscosity distribution in terms of pressure helps in avoiding the occurrence of a curved free-surface or a mixing layer between the channel and porous layer.

For the unidirectional flow at hand, governing equations reduce to the following,

$$\mu_i \frac{d^2 u_i}{dy^2} + \frac{d\mu_i}{dy} \frac{du_i}{dy} + \rho g \sin \vartheta - \sigma \frac{\mu_i}{k} u_i = 0 \quad (3)$$

$$-\frac{dp_i}{dy} - \rho g \cos \vartheta = 0. \quad (4)$$

where when  $i = 1$  and  $\sigma = 1$ , equation (3) represents flow in the porous layer,  $0 \leq y \leq h_1$ , and when  $i = 2$  and  $\sigma = 0$ , equation (3) represent flow in the free-space channel,  $h_1 \leq y \leq h$ .

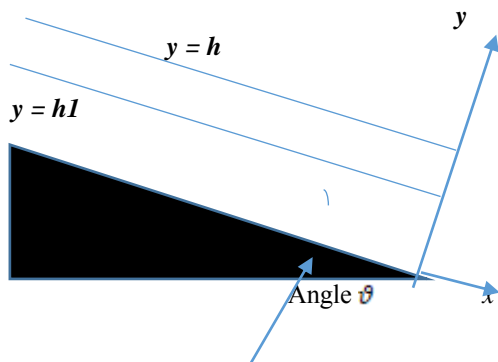


Fig. 1. Representative sketch

At the boundary ( $y = 0$  and  $y = h$ ), the velocity is zero, and the pressure at  $y = h$  is constant  $p_0$ . [13]. The boundary conditions are as follows:

$$u_1(0) = u_2(h) = 0 \quad (5)$$

$$p_2(h) = p_0 \quad (6)$$

At the interface between layers,  $y = h_1$ , velocity, shear stress, viscosity, and pressure are equal and continuous, and take the form:

$$u_1(h_1) = u_2(h_1) \quad (7)$$

$$\mu_1 \frac{du_1}{dy} |_{h_1} = \mu_2 \frac{du_2}{dy} |_{h_1} \quad (8)$$

$$\mu_1(h_1) = \mu_2(h_1) \quad (9)$$

$$p_1(h_1) = p_2(h_1) \quad (10)$$

Following Kannan and Rajagopal, [13], we introduce the following dimensionless quantities with respect to the width of the flow domain,  $h$ , and a characteristic velocity,  $U$ :

$$\bar{y} = \frac{y}{h}; \quad \bar{u}_i = \frac{u_i}{U}; \quad \varepsilon = \frac{h_1}{h}; \quad K = \frac{k}{h^2}; \quad i = 1, 2, \quad (11)$$

where  $0 \leq \bar{y} \leq \varepsilon$  for  $i = 1$ , and  $\varepsilon \leq \bar{y} \leq 1$  for  $i = 2$ .

Equations (3) and (4) take the following forms, respectively:

$$\mu_i \frac{d^2 \bar{u}_i}{d\bar{y}^2} + \frac{d\mu_i}{d\bar{y}} \frac{d\bar{u}_i}{d\bar{y}} + \frac{\rho g h^2 \sin \vartheta}{U} - \sigma \frac{\mu_i}{K} \bar{u}_i = 0 \quad (12)$$

$$\frac{dp_i}{d\bar{y}} = -\rho g h \cos \vartheta \quad (13)$$

and conditions (5)-(10) take the following forms, respectively

$$\bar{u}_1(0) = \bar{u}_2(1) = 0 \quad (14)$$

$$p_2(1) = p_0 \quad (15)$$

$$\bar{u}_1(\varepsilon) = \bar{u}_2(\varepsilon) \quad (16)$$

$$\mu_1 \frac{d\bar{u}_1}{d\bar{y}}(\varepsilon) = \mu_2 \frac{d\bar{u}_2}{d\bar{y}}(\varepsilon) \quad (17)$$

$$\mu_1(\varepsilon) = \mu_2(\varepsilon) \quad (18)$$

$$p_1(\varepsilon) = p_2(\varepsilon) \quad (19)$$

Integrating (13) and using (15) and (19), results in the following pressure distribution across the channel and porous layer:

$$p_i(\bar{y}) = p_0 + (1 - \bar{y})\rho g h \cos \vartheta. \quad (20)$$

Equation (20) represents continuous, and decreasing, pressure functions with values at the interface,  $\bar{y} = \varepsilon$ , and at the lower boundary,  $\bar{y} = 0$ , given respectively, as:

$$p_1(\varepsilon) = p_2(\varepsilon) = p_0 + \rho g h \cos \vartheta (1 - \varepsilon) \quad (21)$$

$$p_1(0) = p_0 + \rho g h \cos \vartheta. \quad (22)$$

In order to solve (12), we first assume that the viscosity in each layer varies with pressure linearly according to the following relationships:

$$\mu_i(p_i) = \alpha p_i \quad (22a)$$

where  $\alpha$  is a positive constant, referred to here as the *viscosity adjustment parameter*. Values of  $\alpha$  are adjustable so that one can avoid unrealistic values of  $\mu_i$ .

We note that viscosity functions (22a) are also decreasing continuous functions of the pressure distributions in each of the channel and porous layer, with  $\mu_1(p_1)$  and  $\mu_2(p_2)$  only being equal when  $p_1 = p_2$ , namely at the interface  $\bar{y} = \varepsilon$ . This implies that condition (18) is met, and permeability at the interface is given by:

$$\mu_1(\varepsilon) = \mu_2(\varepsilon) = \alpha[p_0 + \rho gh \cos\theta (1 - \varepsilon)] \quad (22b)$$

Using (22a), equation (12) takes the following form:

$$p_i^2 \frac{d^2 \bar{u}_i}{d\bar{y}^2} - \beta p_i \frac{d\bar{u}_i}{d\bar{y}} - \sigma \frac{p_i^2}{\kappa} \bar{u}_i = -\gamma p_i \quad (23)$$

where

$$\beta = \rho gh \cos\theta \quad (24)$$

$$\gamma = \frac{\rho gh^2 \sin\theta}{\alpha \nu} \quad (25)$$

We find it advantageous to use the following operators to transform to derivatives with respect to  $p_i$  in order to help select an appropriate function to describe variability in permeability across the porous layer:

$$\frac{d}{d\bar{y}} = -\beta \frac{d}{dp_i} \quad (26)$$

$$\frac{d^2}{d\bar{y}^2} = \beta^2 \frac{d^2}{dp_i^2} \quad (27)$$

Equations (23) can thus be written as:

$$p_i^2 \frac{d^2 \bar{u}_i}{dp_i^2} + p_i \frac{d\bar{u}_i}{dp_i} - \sigma \frac{p_i^2}{\beta^2 \kappa} \bar{u}_i = -\frac{\gamma p_i}{\beta^2} \quad (28)$$

Conditions (14), (16), (17), and (18) take the following forms in terms of  $p$ , respectively:

$$\bar{u}_1(p = p_0 + \beta) = \bar{u}_2(p = p_0) = 0 \quad (29)$$

$$\bar{u}_1(p_0 + \beta(1 - \varepsilon)) = \bar{u}_2(p_0 + \beta(1 - \varepsilon)) \quad (30)$$

$$\mu_1 \frac{d\bar{u}_1}{d\bar{y}}(p_0 + \beta(1 - \varepsilon)) = \mu_2 \frac{d\bar{u}_2}{d\bar{y}}(p_0 + \beta(1 - \varepsilon)) \quad (31)$$

$$\mu_1(p_0 + \beta(1 - \varepsilon)) = \mu_2(p_0 + \beta(1 - \varepsilon)) \quad (32)$$

The form of variable permeability,  $K(\bar{y})$ , appearing in equation (28) needs to be specified. We rely in this work on a variable permeability model developed by Hamdan and Kamel, [31], for flow through a porous layer governed by Brinkman's equation, wherein they suggested a quadratic function of the lateral variable. Considering that the square of the pressure function used in this work is a quadratic function, and that a square of a pressure function chosen for  $K(\bar{y})$  would lead to an analytic solution to equation (28) in terms of elementary functions, we assume that variations in permeability in the porous layer are given by the following decreasing function:

$$K(\bar{y}) = [\delta p_1(\bar{y})]^2; \quad 0 < \bar{y} \leq \varepsilon \quad (33a)$$

where  $\delta$  is a specified *permeability adjustment parameter* whose value can be chosen so that one can avoid unrealistic values of permeability.

Permeability at the interface, is given by

$$K(\varepsilon) = [\delta p(\varepsilon)]^2 \quad (33b)$$

Using (33a), equation (28) reduces to:

$$p_i^2 \frac{d^2 \bar{u}_i}{dp_i^2} + p_i \frac{d\bar{u}_i}{dp_i} - \sigma \frac{1}{\delta^2 \beta^2} \bar{u}_i = -\frac{\gamma p_i}{\beta^2} \quad (34)$$

which has general solutions given by:

$$\bar{u}_1 = c_1 p^{\frac{1}{\delta\beta}} + c_2 p^{-\frac{1}{\delta\beta}} - \frac{\gamma \delta^2}{[\delta^2 \beta^2 - 1]} p \quad (35)$$

$$\bar{u}_2 = d_1 + d_2 \ln p - \frac{\gamma}{\beta^2} p \quad (36)$$

wherein  $c_1, c_2, d_1, d_2$  are arbitrary constants that are determined as follows.

Using conditions (29)-(32) in (35) and (36), yields the following relations between the arbitrary constants:

$$c_1 [\Gamma_1]^{\frac{1}{\delta\beta}} + c_2 [\Gamma_1]^{-\frac{1}{\delta\beta}} = \frac{\gamma \delta^2}{[\delta^2 \beta^2 - 1]} [\Gamma_1] \quad (37)$$

$$d_1 + d_2 \ln p_0 = \frac{\gamma}{\beta^2} p_0 \quad (38)$$

$$c_1 [\Gamma_2]^{\frac{1}{\delta\beta}} + c_2 [\Gamma_2]^{-\frac{1}{\delta\beta}} = d_1 + d_2 \ln [\Gamma_2] - \frac{\gamma}{\beta^2} [\Gamma_2] + \frac{\gamma \delta^2}{[\delta^2 \beta^2 - 1]} [\Gamma_2] \quad (39)$$

$$c_1 (\Gamma_2)^{\frac{1}{\delta\beta}} - c_2 (\Gamma_2)^{-\frac{1}{\delta\beta}} = \delta \beta d_2 - \frac{\gamma \delta \beta \Gamma_2}{\beta^2} + \frac{\gamma \delta^3 \beta \Gamma_2}{[\delta^2 \beta^2 - 1]} \quad (40)$$

Solutions to (37)-(40) are given by:

$$c_1 = \Gamma_9 d_2 + \Gamma_7 \quad (41)$$

$$c_2 = \Gamma_{10} d_2 + \Gamma_8 \quad (42)$$

$$d_1 = -d_2 \ln p_0 + \Gamma_{11} \quad (43)$$

$$d_2 = \frac{2\Gamma_6}{\Gamma_5} \quad (44)$$

where

$$\Gamma_1 = p_0 + \beta \quad (45)$$

$$\Gamma_2 = p_0 + \beta(1 - \varepsilon) \quad (46)$$

$$\Gamma_3 = \left[ \frac{\Gamma_2}{\Gamma_1} \right]^{\frac{1}{\delta\beta}} + \left[ \frac{\Gamma_1}{\Gamma_2} \right]^{\frac{1}{\delta\beta}} \quad (47)$$

$$\Gamma_4 = \left[ \frac{\Gamma_2}{\Gamma_1} \right]^{\frac{1}{\delta\beta}} - \left[ \frac{\Gamma_1}{\Gamma_2} \right]^{\frac{1}{\delta\beta}} \quad (48)$$

$$\Gamma_5 = -\delta\beta\Gamma_4 + \Gamma_3 \ln \left[ \frac{\Gamma_2}{p_0} \right] \quad (49)$$

$$\Gamma_6 = \frac{\gamma\delta^2}{[\delta^2\beta^2 - 1]} [\Gamma_1] - \frac{\gamma}{2\beta^2} [p_0 - \Gamma_2] \Gamma_3 - \frac{\gamma\delta^2\Gamma_2}{2[\delta^2\beta^2 - 1]} (\Gamma_3 - \beta\delta\Gamma_4) - \frac{\gamma\delta\Gamma_2}{2\beta} \Gamma_4 \quad (50)$$

$$\Gamma_7 = [\Gamma_2]^{-\frac{1}{\delta\beta}} \left\{ \frac{\gamma}{2\beta^2} [p_0 - \Gamma_2] + \frac{\gamma\delta^2\Gamma_2}{2[\delta^2\beta^2 - 1]} (1 + \beta\delta) - \frac{\gamma\delta\Gamma_2}{2\beta} \right\} \quad (51)$$

$$\Gamma_8 = [\Gamma_2]^{\frac{1}{\delta\beta}} \left\{ \frac{\gamma}{2\beta^2} [p_0 - \Gamma_2] + \frac{\gamma\delta^2\Gamma_2}{2[\delta^2\beta^2 - 1]} (1 - \beta\delta) + \frac{\gamma\delta\Gamma_2}{2\beta} \right\} \quad (52)$$

$$\Gamma_9 = \frac{1}{2} (\delta\beta + \ln \left[ \frac{\Gamma_2}{p_0} \right]) [\Gamma_2]^{-\frac{1}{\delta\beta}} \quad (53)$$

$$\Gamma_{10} = \frac{1}{2} (-\delta\beta + \ln \left[ \frac{\Gamma_2}{p_0} \right]) [\Gamma_2]^{\frac{1}{\delta\beta}} \quad (54)$$

$$\Gamma_{11} = \frac{\gamma}{\beta^2} p_0 \quad (55)$$

With the knowledge of the velocity distributions (35) and (36) in the porous layer and in the channel, respectively, we obtain the following expressions for the vorticities,  $\omega_i$ , and shear stresses,  $\tau_i$ , for  $i=1,2$ , in the porous layer and in the channel, respectively:

$$\omega_1 = -\frac{du_1}{dy} = -\left[ -\beta \frac{du_1}{dp} \right] = \beta \frac{du_1}{dp} = c_1 \frac{1}{\delta} p^{\frac{1}{\delta\beta}-1} - c_2 \frac{1}{\delta} p^{-\frac{1}{\delta\beta}-1} - \frac{\gamma\delta^2}{\beta[\delta^2\beta^2 - 1]} \quad (56)$$

$$\tau_1 = \mu_1 \frac{d\bar{u}_1}{d\bar{y}} = -\beta \mu_1 \frac{du_1}{dp} = -\mu_1(p) \left[ c_1 \frac{1}{\delta} p^{\frac{1}{\delta\beta}-1} - c_2 \frac{1}{\delta} p^{-\frac{1}{\delta\beta}-1} - \frac{\gamma\delta^2}{\beta[\delta^2\beta^2 - 1]} \right] \quad (57)$$

$$\omega_2 = -\frac{du_2}{dy} = \beta \frac{du_2}{dp} = \beta \frac{d_2}{p} - \frac{\gamma}{\beta} \quad (58)$$

$$\tau_2 = \mu_2 \frac{d\bar{u}_2}{d\bar{y}} = -\beta \mu_2 \frac{du_2}{dp} = -\mu_2 \left[ \beta \frac{d_2}{p} - \frac{\gamma}{\beta} \right] \quad (59)$$

Using (35), (36), and (56)-(59), we obtain the following expressions for velocity, vorticity and shear stress, respectively, at the interface,  $\bar{y} = \varepsilon$ :

$$\bar{u}_1(y = \varepsilon) = c_1 [\Gamma_2]^{\frac{1}{\delta\beta}} + c_2 [\Gamma_2]^{-\frac{1}{\delta\beta}} - \frac{\gamma\delta^2}{[\delta^2\beta^2 - 1]} \Gamma_2 \quad (60)$$

$$\bar{u}_2(y = \varepsilon) = d_1 + d_2 \ln \Gamma_2 - \frac{\gamma}{\beta^2} \Gamma_2 \quad (61)$$

$$\omega_1(\varepsilon) = c_1 \frac{1}{\delta} (\Gamma_2)^{\frac{1}{\delta\beta}-1} - c_2 \frac{1}{\delta} (\Gamma_2)^{-\frac{1}{\delta\beta}-1} - \frac{\gamma\delta^2}{\beta[\delta^2\beta^2 - 1]} \quad (62)$$

$$\omega_2(\varepsilon) = \beta \frac{d_2}{\Gamma_2} - \frac{\gamma}{\beta} \quad (63)$$

$$\tau_1(\varepsilon) = -\mu_1(\Gamma_2) \left[ c_1 \frac{1}{\delta} (\Gamma_2)^{\frac{1}{\delta\beta}-1} - c_2 \frac{1}{\delta} (\Gamma_2)^{-\frac{1}{\delta\beta}-1} - \frac{\gamma\delta^2}{\beta[\delta^2\beta^2 - 1]} \right] \quad (64)$$

$$\tau_2(\varepsilon) = -\mu_2 \left[ \beta \frac{d_2}{\Gamma_2} - \frac{\gamma}{\beta} \right] \quad (65)$$

### 3. Results and Analysis

#### 3.1 Ranges of Parameters

Following Kannan and Rajagopal, [13], we take  $\rho g = 1$  and  $h = 1$ . We further take  $U = 10$  as a representative characteristic velocity. The following ranges of parameters are also considered as representative of the media and flow quantities:

Range of inclination angle  $\vartheta$ : 30, 60, 75 degrees

Range of  $p_0$ : 2, 3, 5

Range of  $\varepsilon$ : 0.25, 0.5, 0.75

Range of  $\delta$ : 1, 0.5, 0.1, 0.05, 0.02

Range of  $\alpha$ : 0.1, 1, 2

#### 3.2 Pressure and Viscosity Distributions:

Pressure distribution in the porous layer and in the channel are given by equation (20). At the interface between the channel and porous layer, pressure is given by equation (21). Pressure distribution is represented across the channel and porous layer by a single, continuous and decreasing function. This function is not influenced by the porous layer thickness, but is dependent on the pressure condition  $p_0$  and the angle of inclination. However, the value of pressure at the interface depends on the value of  $\varepsilon$  as well, as can be seen from equation (21).

Dependence of pressure on the angle of inclination, for a given  $p_0$ , is illustrated in **Fig. 2(a)**. Dependence of pressure on  $p_0$  for a given angle of inclination, is illustrated in **Fig. 2(b)**. Both figures show the linear decrease of the pressure function across the flow configuration. For smaller angles of inclination, **Fig. 2(b)**, shows higher pressure at the lower boundary and the interface between the porous layer and the

channel. For higher values of  $p_0$ , Fig. 2(b). shows higher pressure at the lower boundary and at the interface.

Viscosity distribution is given by equations (22a) and viscosity at the interface is given by (22b). Since viscosity is proportional to pressure in the current model with a constant of proportionality,  $\alpha$ , graphs of viscosity and pressure distributions are the same when  $\alpha = 1$ .

### 3.3 Permeability Distribution:

Permeability distribution in the porous layer is given by equation (33a), and depends on multiplier  $\delta$ , on  $p_0$ , and on the porous layer thickness (by virtue of dependence of permeability on pressure at the interface). At the interface,  $y = \varepsilon$ , permeability is given by (33b)

Dependence of permeability function on the multiplier  $\delta$  is illustrated in Fig. 3(a), for  $\delta = 1, 0.5$  and  $0.1$ . For the given pressure distribution when  $P_0 = 2$  and angle of inclination  $\vartheta = 30^\circ$ , shown in Fig. 2(a) and Fig. 2(b), the permeability distribution is either the square of the pressure, when  $\delta = 1$ , or scaling of the square of pressure, when  $0 < \delta < 1$ . The relative scaling is shown in Fig. 3(a) to decrease the permeability with decreasing  $\delta$ .

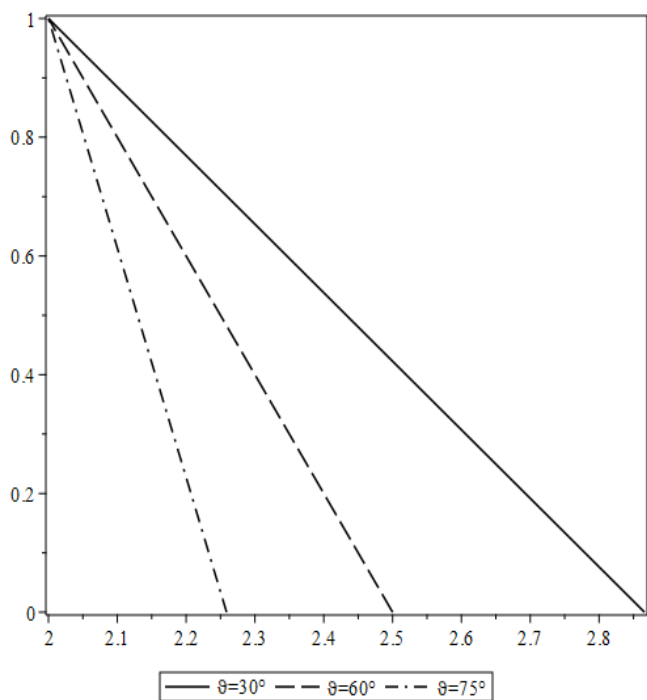


Fig. 2(a). Pressure Distribution for different  $\vartheta$ .  
 $P_0 = 2, U = 10$ .

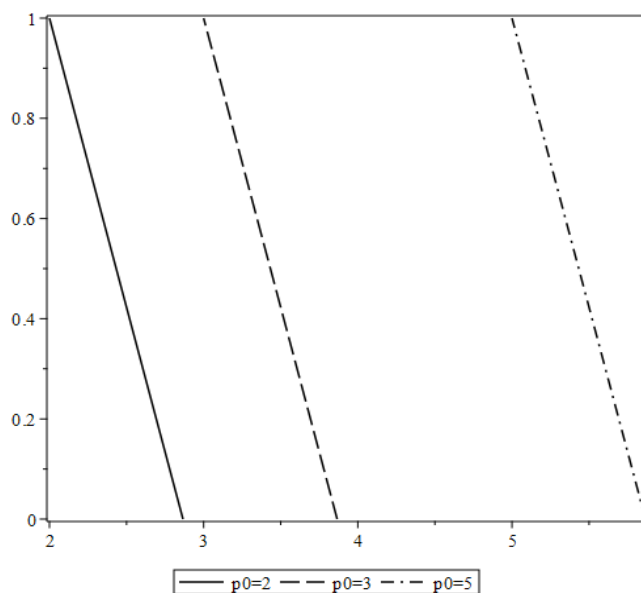


Fig. 2(b). Pressure Distribution different  $P_0$ .  
 $\vartheta = 30^\circ, U = 10$

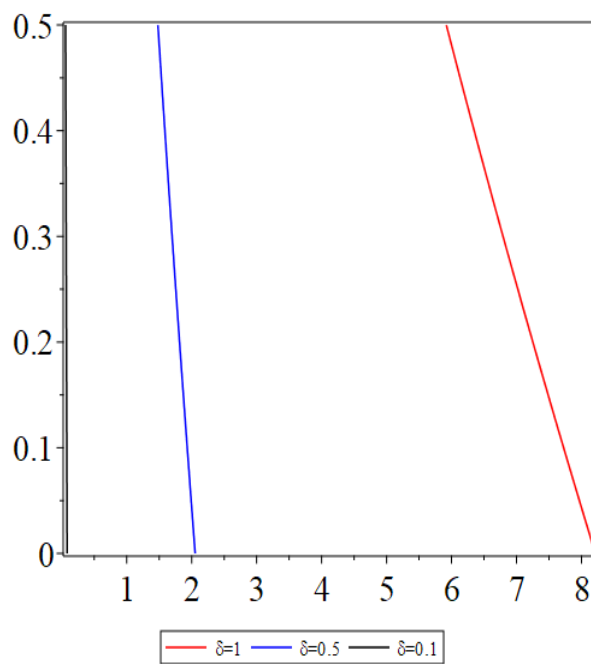
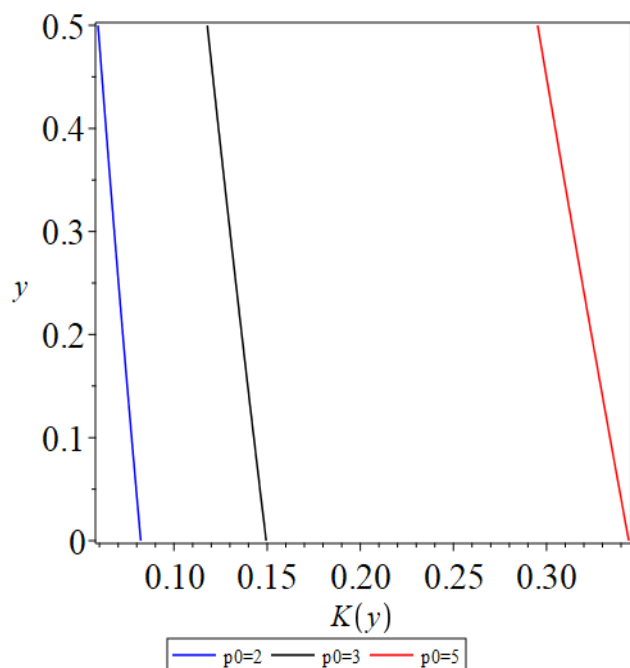


Fig. 3(a). Permeability Distribution for various values of  $\delta$ .  
 $\vartheta = 30, \varepsilon = 0.5, P_0 = 2, U = 10$ .

Dependence of permeability function on  $p_0$  is illustrated in Fig. 3(b) when  $\delta = 0.1$ , and in Fig. 3(c) when  $\delta = 0.02$ . Both figures demonstrate the relative decrease in permeability with decreasing  $P_0$ , for a given angle of inclination, porous layer thickness,  $\varepsilon$ , and parameter  $\delta$ . This is due to the fact that decreasing  $P_0$  has the effect of decreasing pressure in the porous layer, with the net result of decreasing permeability. Furthermore, decreasing  $\delta$  from  $\delta = 0.1$  to  $\delta = 0.02$  results in decreasing permeability twenty five-fold (or by a factor of  $(\frac{0.1}{0.02})^2 = 25$ ).

Dependence of permeability function on angle of inclination is illustrated in **Fig. 3(d)**, when  $\delta = 0.1$ , and **Fig. 3(e)**, when  $\delta = 0.02$ . Since the variable permeability function is defined to be proportional to the square of the pressure function, and pressure decreases with increasing angle of inclination, therefore increasing angle of inclination results in decreasing permeability. This is demonstrated in both **Fig. 3(d)** and **Fig. 3(e)**, which also show the effect of decreasing parameter  $\delta$  on substantially decreasing permeability.



**Fig. 3(b).** Permeability Distribution for various values of  $P_0$ .  
 $\vartheta = 30^\circ, \delta = 0.1, \varepsilon = 0.5, U = 10$

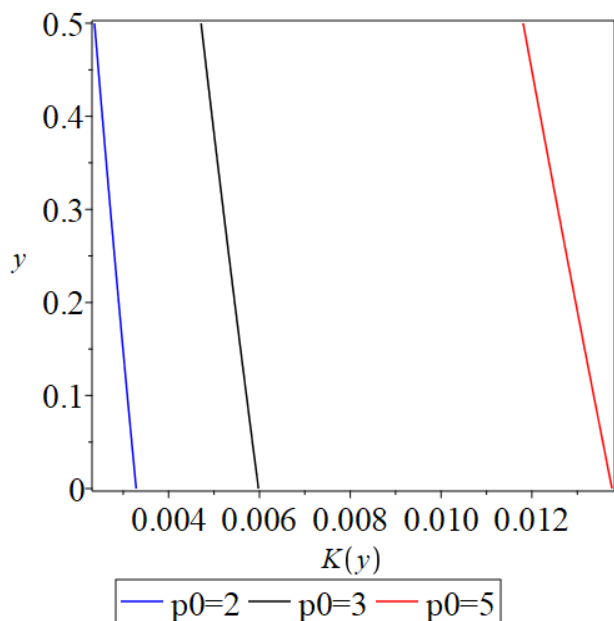


**Fig. 3(c).** Permeability Distribution for various values of  $P_0$ .  
 $\vartheta = 30^\circ, \delta = 0.02, \varepsilon = 0.5, U = 10$

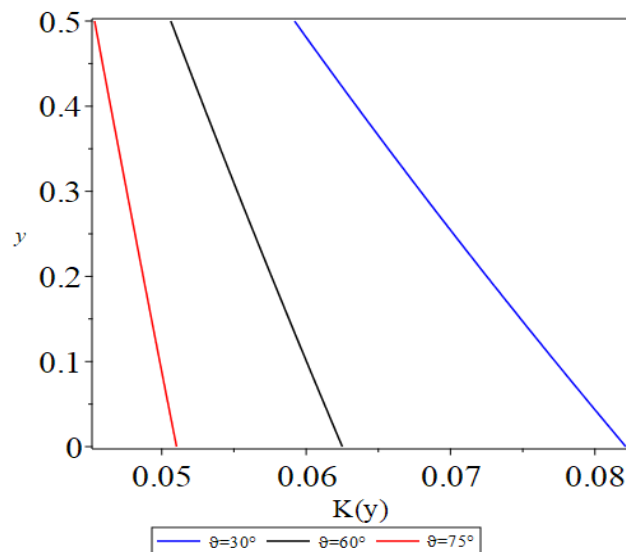


**Fig. 3(d).** Permeability Distribution for different angles of inclination.  
 $\delta = 0.1, P_0 = 2, \varepsilon = 0.5, U = 10$

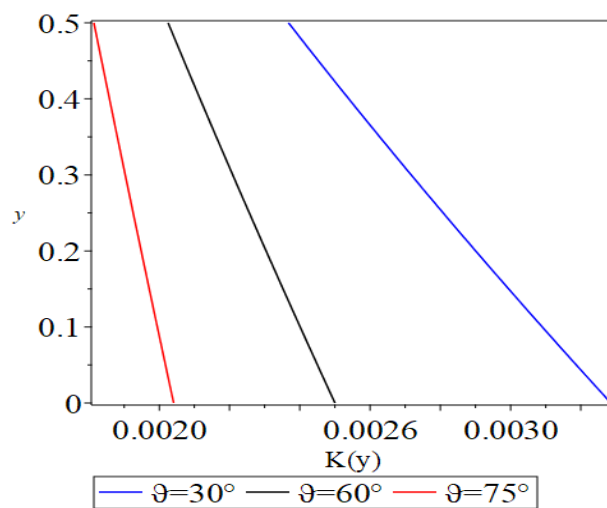


**Fig. 3(e).** Permeability Distribution for different angles of inclination.  
 $\delta = 0.02, P_0 = 2, \varepsilon = 0.5, U = 10$

### 3.4 Velocity Profiles

Velocities in the porous layer and the channel are given by equations (35) and (36), respectively. Effects of the various flow and medium parameters on the velocity profiles are discussed in what follows.

#### Effects of $\delta$

Permeability function is defined in this work to be proportional to the square of pressure function, with the constant of proportionality  $\delta^2$ . For a given pressure distribution in the porous layer, permeability increases with

increasing  $\delta$ . When  $\delta = 1$ , permeability is high and the flow through the porous layer resembles the flow in the free-space channel, and the velocity profile across the flow domain is parabolic. As  $\delta$  decreases, velocity in the porous layer decreases and results in a non-parabolic profile, as illustrated in Fig. 4(a).

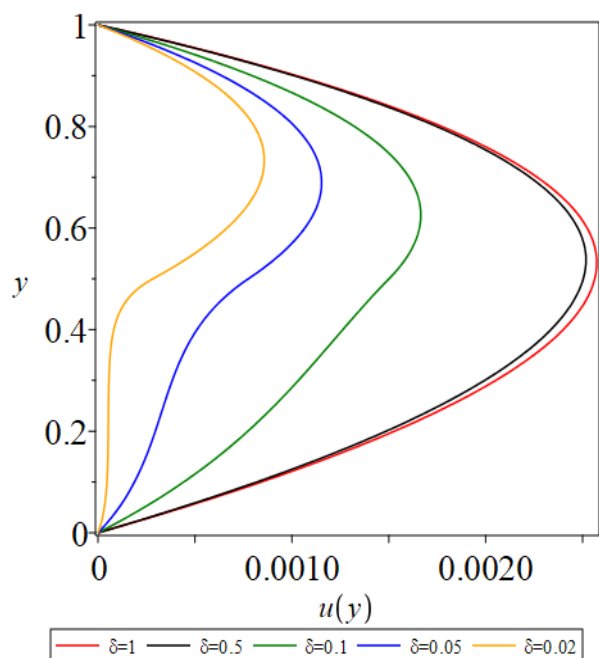


**Fig. 4(a).** Velocity Profile for different values of  $\delta$ .  
 $\varepsilon = 0.5, \vartheta = 30$  and  $\alpha = 1, p_0 = 2, \delta = 1, U = 10$ .

*Effects of  $\alpha$*

For a given pressure distribution, increasing  $\alpha$  results in increasing viscosity without a change in permeability. Increasing viscosity results in slowing down the flow in the channel and, for a given permeability, in the porous layer. This is illustrated in Fig. 4(b) which shows the slowing down of the flow when  $\alpha$  increases.

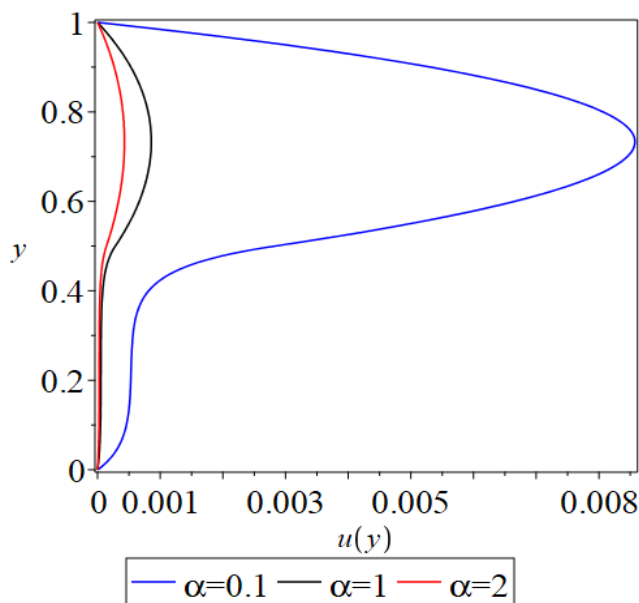


**Fig. 4(b).** Velocity Profile for different values of  $\alpha$

$$\varepsilon = 0.5, \vartheta = 30, p_0 = 2, \delta = 0.02, U = 10.$$

*Effects of  $p_0$*

**Fig. 4(c)** illustrates the effects of  $p_0$  on the velocity profile. It shows that in the porous layer, decreasing  $p_0$  results in decreasing the velocity due to the fact that permeability decreases in the porous layer. In the channel, however, decreasing  $p_0$  results in increasing the velocity due to the decrease in viscosity associated with decreasing  $p_0$ , and less resistance to the flow is offered.

*Effects of  $\vartheta$*

Associated with increasing angle of inclination is a decrease in the pressure distribution, hence a decrease in viscosity and permeability distributions. The effects of this increase on velocity profile is as follows. In the free-space channel, a decrease in viscosity due to a decrease in pressure results in increasing velocity with increasing inclination angle. This results in higher momentum transfer, and greater influence on the flow in the porous layer. In the porous layer, there is a decrease in permeability with increasing angle of inclination, and one expects a slower flow. However, there is an associated decrease in viscosity and the influence of momentum transfer from the channel, which overcome the decrease in velocity due to permeability decrease. The net result is that across the configuration, velocity increases with increasing angle of inclination, as shown in Fig. 4(d).

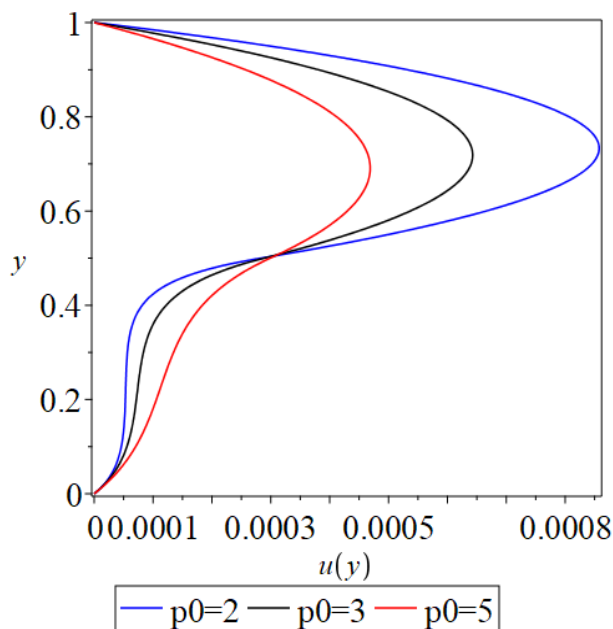


**Fig. 4(c).** Velocity Profile for different  $p_0$   
 $\varepsilon = 0.5, \vartheta = 30, \alpha = 1, \delta = 0.02, U = 10$ .

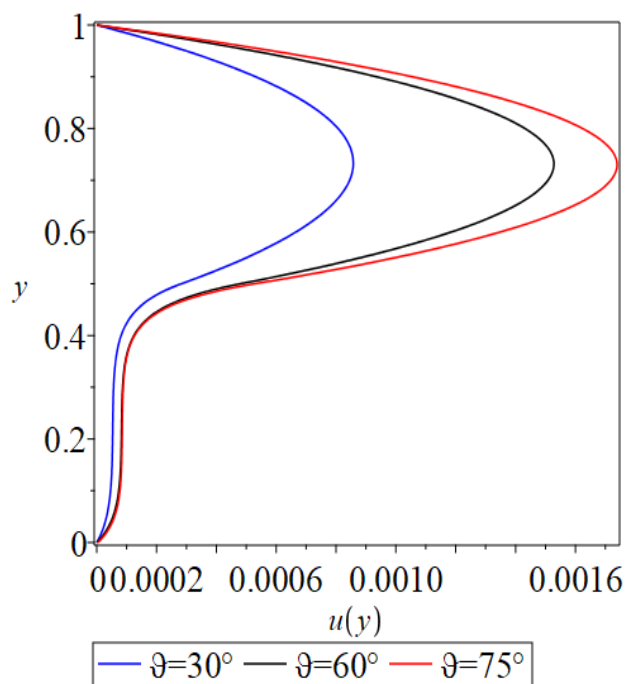


Fig. 4(d). Velocity Profile for different angles of inclination.  
 $\varepsilon = 0.5, \alpha = 1, p_0 = 2, \delta = 0.02, U = 10.$

### 3.5 Values at the Interface

Velocity, vorticity and shear stress at the interface  $\bar{y} = \varepsilon$  are tabulated below for different parameters using expressions (60)-(65).

Tables 1 through 6 illustrate velocity, vorticity and shear stress at the interface for different parameters. Table 1 illustrates the effects of  $\delta$  on interfacial quantities and show the expected decrease of velocity at the interface with decreasing  $\delta$ . This behaviour is in line with the effects of  $\delta$  on the velocity profile, shown in Fig. 4(a). Vorticity and shear stress at the interface increase, in magnitude, with decreasing  $\delta$ . This is also in line with the velocity profiles depicted in Fig. 4(a) if one considers the behaviour of slopes of the velocity curves at the interface  $y = \varepsilon$ .

Table 1: Velocity, vorticity, and shear stress at the interface for different  $\delta$ .  
 $\varepsilon = 0.5, \text{ and } \vartheta = 30, \alpha = 1, p_0 = 2, U = 10.$

$\delta$	$\bar{u}_1(y = \varepsilon)$	$\omega_1(y = \varepsilon)$	$\tau_1(y = \varepsilon)$
1	0.0025621911	-0.0006518773	0.0015860257
0.5	0.00250312451	-0.0007591557	0.0018470354
0.1	0.0015008312	-0.0025795374	0.0062760472
0.05	0.00077518572	-0.0038974667	0.0094825861
0.02	0.00028268658	-0.0047919517	0.0116588793

Also in line with the velocity profile figures, Fig. 4(a) to Fig. 4(d), are the effects of the parameters  $\varepsilon, \alpha, \vartheta$  and  $p_0$  on the velocity at the interface, illustrated in Tables 2, 3, 4 and 5.

These tables also document the values of vorticity and shear stress at the interface. We summarize their effects as follows.

Increasing the porous layer thickness,  $\varepsilon$ , results in a decrease in the interfacial velocity, and a corresponding decrease in the magnitude of vorticity and shear stress at the interface, as shown in Table 2.

Increasing  $p_0$  results in an increase in the interfacial velocity, and a decrease in the magnitude of vorticity and shear stress at the interface, as shown in Table 3.

Increasing  $\alpha$  results in a decrease in the interfacial velocity and a decrease in the magnitude of vorticity, but has no effect on the value of shear stress at the interface, as shown in Table 4.

Increasing the angle of inclination,  $\vartheta$ , results in an increase in the interfacial velocity, and a corresponding increase in the magnitude of vorticity and shear stress at the interface, as shown in Table 5.

Table 2: Velocity, vorticity, and shear stress at the interface for different  $\varepsilon$ .

$$\vartheta = 30^\circ, \alpha = 1, p_0 = 2, \delta = 0.02, U = 10$$

$\varepsilon$	$\bar{u}_1(y = \varepsilon)$	$\omega_1(y = \varepsilon)$	$\tau_1(y = \varepsilon)$
0.25	0.000419337	-0.006920644	0.018336379
0.5	0.000282687	-0.004791952	0.011658879
0.75	0.000147412	-0.002307693	0.005115017

Table 3: Velocity, vorticity, and shear stress at the interface for different  $p_0$ .

$$\varepsilon = 0.5, \text{ and } \vartheta = 30, \alpha = 1, \delta = 0.02, U = 10.$$

$p_0$	$\bar{u}_1(y = \varepsilon)$	$\omega_1(y = \varepsilon)$	$\tau_1(y = \varepsilon)$
2	0.0002826866	-0.004791952	0.011658879
3	0.0002882884	-0.003183514	0.010929043
5	0.0002988539	-0.001759034	0.009556856

Table 4: Velocity, vorticity, and shear stress at the interface for different  $\alpha$ .

$$\varepsilon = 0.5, \text{ and } \vartheta = 30, p_0 = 2, \delta = 0.02, U = 10.$$

$\alpha$	$\bar{u}_1(y = \varepsilon)$	$\omega_1(y = \varepsilon)$	$\tau_1(y = \varepsilon)$
0.1	0.00282686584	-0.04791952	0.0116588793
1	0.00028268658	-0.0047919517	0.0116588793
2	0.00014134328	-0.0023959758	0.0116588793

Table 5: Velocity, vorticity, and shear stress at the interface for different  $\vartheta$ .

$$\varepsilon = 0.5, \text{ and } \alpha = 1, p_0 = 2, \delta = 0.02, U = 10.$$

$\vartheta$	$\bar{u}_1(y = \varepsilon)$	$\omega_1(y = \varepsilon)$	$\tau_1(y = \varepsilon)$
30	0.0002826866	-0.004791952	0.01165887927
60	0.0004795235	-0.008906635	0.02003992785
75	0.0005271848	-0.010436801	0.02222422446

## 4. Conclusion

In this work, we considered the coupled, parallel flow of a fluid with pressure-dependent viscosity through an inclined free-space channel over a Brinkman-type porous layer, of variable permeability and variable thickness, and saturated by the same fluid. Pressure variations through the flow domain were described by a continuous linear function. Viscosity was expressed as a continuous, linear function of pressure, while permeability in the porous layer was expressed in terms of a quadratic function that is proportional to the square of the linear pressure function. Model equations were solved subject to continuity of velocity, pressure, viscosity and shear stress at the interface, and the no-slip condition on solid boundaries. Results obtained support the following conclusions:

- 1) The most important parameters influencing the flow are the angle of inclination,  $\vartheta$ , pressure condition  $p_0$  at the upper channel wall, thickness  $\varepsilon$  of the porous layer, permeability adjustment parameter  $\delta$  of equation (33a), and the viscosity adjustment parameter  $\alpha$  of equation (22a).
- 2) The most sensitive of the parameters in part (a), above, are  $\alpha$  and  $\delta$  as they control the permeability and viscosity distributions for a given pressure distribution. High values of  $\delta$  result in unrealistic variable permeability distribution. High and low values of  $\alpha$  could result in unrealistic viscosity values.
- 3) Effects of the parameters on velocity at the interface are as follows:
  - 1.1) Increasing  $\vartheta$ , all other parameters fixed, increases the velocity at the interface.
  - 1.2) Increasing  $\delta$ , all other parameters fixed, increases the velocity at the interface.
  - 1.3) Increasing  $p_0$ , all other parameters fixed, increases the velocity at the interface.
  - 1.4) Increasing  $\alpha$ , all other parameters fixed, decreases the velocity at the interface.
  - 1.5) Increasing  $\varepsilon$ , all other parameters fixed, decreases the velocity at the interface.

## References

[1] M. Lanzendörfer, "On steady inner flows of an incompressible fluid with the viscosity depending on the pressure and the shear rate", *Nonlinear Analysis: Real World*

Applications, vol. 10, pp. 1943-1954, 2009.

[2] K.B. Nakshatrala and K.R. Rajagopal, "A numerical study of fluids with pressure-dependent viscosity flowing through a rigid porous medium", *Int. J. Numer. Meth. Fluids*, vol. 67, pp. 342-368, 2011.

[3] K.R. Rajagopal, G. Saccomandi and L. Vergori, "Flow of fluids with pressure- and shear-dependent viscosity down an inclined plane", *J. Fluid Mechanics*, vol. 706, pp. 173-189, 2012.

[4] A.Z. Szeri, "Fluid Film Lubrication: Theory and Design", Cambridge University Press, 1998.

[5] A.K. Singh, P.K. Sharma and N.P. Singh, "Free convection flow with variable viscosity through horizontal channel embedded in porous medium", *The Open Applied Physics Journal*, vol. 2, pp. 11-19, 2009.

[6] F.J. Martinez-Boza, M.J. Martin-Alfonso, C. Callegos and M. Fernandez, "High-pressure behavior of intermediate fuel oils", *Energy Fuels*, vol. 25, pp. 5138-5144, 2011.

[7] G.G. Stokes, "On the theories of the internal friction of fluids in motion, and of equilibrium and motion of elastic solids", *Trans. Camb. Philos. Soc.*, vol. 8, pp. 287-305, 1845.

[8] C.J. Barus, "Note on dependence of viscosity on pressure and temperature", *Proceedings of the American Academy*, vol. 27, pp. 13-19, 1891.

[9] C.J. Barus, "Isothermals, isopiestic and isometrics relative to viscosity", *American Journal of Science*, vol. 45, pp. 87-96, 1893.

[10] P.W. Bridgman, "The Physics of High Pressure", MacMillan, New York, 1931.

[11] P.H. Vergne, "Pressure viscosity behavior of various fluids", *High Press. Res.*, vol. 8, pp. 451-454, 1991.

[12] S.C. Subramanian and K.R. Rajagopal, "A note on the flow through porous solids at high Pressures", *Computers and Mathematics with Applications*, vol. 53, pp. 260-275, 2007.

[13] K. Kannan and K.R. Rajagopal, "Flow through porous Media due to high pressure gradients", *J. Applied Mathematics and Computation*, vol. 199, pp. 748-759, 2008.

[14] J. Málek, J. Necas and K.R. Rajagopal, "Global existence of solutions for flows of fluids with pressure and shear dependent viscosities", *Applied Mathematics Letters*, vol. 15, pp. 961-967, 2002.

[15] L. Fusi, A. Farina and F. Rosso, "Mathematical models for fluids with pressure-dependent viscosity flowing in porous media", *Int. Journal of Engineering Science*, vol. 87, pp. 110-118, 2015.

[16] S. Srinivasan and K.R. Rajagopal, "A thermodynamic basis for the derivation of the Darcy, Forchheimer and Brinkman models for flows through porous media and their generalizations", *Int. J. of Non-Linear Mechanics*, vol. 58, pp. 162-166, 2014.

[17] J. Chang, K.B. Nakashatrala and J.N. Reddy, "Modification to Darcy-Forchheimer model due to pressure-dependent viscosity: consequences and numerical solutions", *J. Porous Media*, vol. 20(3), pp. 263-285, 2017.

- [18] M.S. Abu Zaytoon, F.M. Allan, T.L. Alderson and M.H. Hamdan, "Averaged equations of flow of fluid with pressure-dependent viscosity through porous media", *Elixir Appl. Math.*, vol. 96, pp. 41336-41340, 2016.
- [19] K.D. Housiadas and G.C. Georgiou, "New analytical solutions for weakly compressible Newtonian Poiseuille flows with pressure-dependent viscosity", *Int. J. of Engineering Science*, vol. 107, pp. 13-27, 2016.
- [20] K.D. Housiadas, G.C. Georgiou and R.I. Tanner, "A note On the unbounded creeping flow past a sphere for Newtonian fluids with pressure-dependent viscosity", *Int. J. of Engineering Science*, vol. 86, pp. 1-9, 2015.
- [21] G.A. Danish, M. Imran, C. Fetecau and D. Vieru, "First exact solutions for mixed boundary value problems concerning the motions of fluids with exponential dependence of viscosity on pressure", *AIP Advances*, vol. 10, 065206, 2020.
- [22] J. Hron, J. Malek and K.R. Rajagopal, "Simple flows of fluids with pressure-dependent viscosities", *Proceedings of the Royal Society*, vol. 457, pp. 1603-1622, 2001.
- [23] J. Málek and K.R. Rajagopal, "Mathematical issues concerning the Navier-Stokes equations and some of its generalizations", In: *Handbook of Differential Equations: Evolutionary Equations*, Elsevier/North Holland, vol. 2, pp. 371-459, 2005.
- [24] J. Málek and K.R. Rajagopal, "Mathematical properties of the solutions to the equations governing the flow of fluids with pressure and shear rate dependent viscosities", In: *Handbook of Mathematical Fluid Dynamics*, Elsevier, pp. 407-444, 2007.
- [25] V.L. Savatorova and K.R. Rajagopal, "Homogenization of a generalization of Brinkman's equation for the flow of a fluid with pressure dependent viscosity through a rigid porous solid", *ZAMM*, vol. 91(8), pp. 630-648, 2011.
- [26] S. Srinivasan, A. Bonito and K.R. Rajagopal, "Flow of a fluid through a porous solid due to high pressure gradient", *Journal of Porous Media*, vol. 16, pp. 193-203, 2013.
- [27] S.M. Alzahrani, I. Gadoura and M.H. Hamdan, "Flow down an inclined plane of a fluid with pressure-dependent viscosity through a porous medium with constant permeability", *Journal of Modern Technology and Engineering*, vol. 2(2), pp. 155-166, 2017.
- [28] S.M. Alzahrani, I. Gadoura and M.H. Hamdan, "A note on the flow of a fluid with pressure-dependent viscosity through a porous medium with variable permeability", *J. of Modern Technology and Engineering*, vol. 2(1), pp. 21-33, 2017.
- [29] C. Pozrikidis, "Multifilm flow down an inclined plane: Simulations based on the lubrication approximation and normal-mode decomposition of linear waves", In: *Fluid Dynamics at Interfaces*, pp. 112-128, Wei Shyy and R. Narayanan eds. Cambridge University Press, 1999.
- [30] N. Rudraiah, "Coupled parallel flows in a channel and a bounding porous medium of finite thickness", *J. Fluids Engineering, ASME*, vol. 107, pp. 322-329, 1985.
- [31] M.H. Hamdan and M.T. Kamel, "Flow through variable permeability porous layers", *Adv. Theor. Appl. Mech.*, vol. 4(3), pp. 135-145, 2011.

### Contribution of individual authors to this work

Both authors participated in pertinent literature review to identify what has been accomplished in this field, and what state-of-the-art knowledge in this area of research is needed.

Both authors independently obtained the solutions to governing equations.

M.S. Abu Zaytoon outlined the steps to take in conducting this research.

M.S. Abu Zaytoon provided calculations and graphing of results using *Maple*, and provided initial analysis of results.

M.H. Hamdan identified what quantities to calculate and values of parameters to be used.

M.H. Hamdan analysed the results wrote the manuscript.

### Sources of funding

This research did not receive any specific grant from funding agencies in the public, commercial, or not-for-profit sectors.

### Declaration of Competing Interests

The authors declare no competing or conflict of interests in conducting this original research. Neither of the authors stands to gain financially from this work.

### Creative Commons Attribution License 4.0 (Attribution 4.0 International , CC BY 4.0)

This article is published under the terms of the Creative Commons Attribution License 4.0

[https://creativecommons.org/licenses/by/4.0/deed.en\\_US](https://creativecommons.org/licenses/by/4.0/deed.en_US)